







Spin crossover behaviour of asymmetrical iron(III) Schiff base complexes from ethylenediamine†

Dawit Tesfaye, ^{abcd} Mamo Gebrezgiabher, ^{ab} Jonas Braun, ^e Taju Sani,^{ab} Abbasher Gismelseed,^f Tim Hochdörffer,^g Volker Schünemann, ^g Juraj Kuchár, ^d Juraj Černák, ^d Christopher E. Anson, ^e Madhu Thomas ^{*ab} and Annie K. Powell ^{*e}

Novel asymmetrical Fe(III) Schiff base coordination complexes, with the N₄O₂ coordination environment, exhibiting abrupt spin crossover (SCO) behaviour with a wide hysteresis loop of 27 K, have been synthesised from an ethylenediamine based asymmetrical Schiff base ligand viz. *N*-(2-amino-ethyl)salicylaldimine (saen) and characterised via single crystal XRD measurements, variable temperature magnetic studies and Mössbauer measurements. The single crystal XRD measurements prove that the compound is a mixture of two fractions, one with methanol and the other without methanol, viz. [Fe(saen)₂]NO₃·CH₃OH at 299 K (**1–299**) and at 173 K (**1–173**) and [Fe(saen)₂]NO₃ at 173 K (**2–173**), confirming that the Fe(III) centre has a distorted octahedral coordination geometry having two deprotonated asymmetrical tridentate saen ligands, counterbalanced by a nitrate anion and methanol solvent molecule in **1** while **2** has a non-solvate form. An extended hydrogen bonding network between the amino hydrogen atoms of the saen ligand, nitrate counteranion, and methanol solvate molecule is observed in fraction **1**, while an extended zig-zag hydrogen bonding between the nitrate anion and amino hydrogens of saen is observed in fraction **2**. Furthermore, the complex has been characterised by variable temperature magnetic susceptibility measurements and ⁵⁷Fe Mössbauer spectroscopy, confirming the SCO nature.

Introduction

Ever since the first discovery of spin crossover (SCO) compounds,¹ this spectacular class of compounds using a variety of d⁴–d⁷ transition metal ions has drawn the attention of many

investigators. The phenomenon of SCO occurs due to the near equivalence of ligand field splitting and spin-pairing energy. The transition from the high spin (HS) to the low spin (LS) state can be triggered by external stimuli such as temperature, pressure, magnetic fields or light.^{2–5} Depending on the ligand field and other factors such as hydrogen bonding, lattice solvents and counterions, various types of SCO transitions can be possible, exhibiting gradual and abrupt transition with or without hysteresis, two-step transition with plateau or incomplete transitions.^{6,7} Among these, in particular, bistable SCO compounds with sharp with open hysteresis having a $\Delta T \geq 45$ K around room temperature are desirable for various applications.^{6,7}

Schiff bases, also known as imines or azomethines, are the condensation products of the reaction of primary amines with carbonyl compounds.⁸ The richness of Schiff base chemistry is based on the fact that it brings the desired coordination sites together by a simple imine condensation for the design and synthesis of intended coordination compounds with both 3d and 4f metal ions.^{9,10} In our recent reviews, we have shown the effectiveness of Schiff base ligands in preparing lanthanide-based single molecule magnets and iron(II) SCO compounds for possible memory device application.^{6,7,10,11}

In iron SCO chemistry, Fe(II) complexes have been more often reported than Fe(III) due to their propensity to exhibit

^a Department of Industrial Chemistry, College of Natural and Applied Sciences, Addis Ababa Science and Technology University, Addis Ababa P.O. Box 16417, Ethiopia. E-mail: madhu.thomas@aastu.edu.et

^b Nanotechnology Center of Excellence, Addis Ababa Science and Technology University, Addis Ababa P.O. Box 16417, Ethiopia

^c Department of Chemistry, College of Natural Sciences, Salale University, Fitche P.O.Box 245, Ethiopia

^d Department of Inorganic Chemistry, Institute of Chemistry, P. J. Šafárik University in Košice, Moyzesova 11, 041 54 Košice, Slovakia

^e Institute of Inorganic Chemistry (AOC), Institute of Nanotechnology (INT) and Institute for Quantum Materials and Technologies (IQMT) Karlsruhe Institute of Technology (KIT), Kaiserstr. 12, 76131 Karlsruhe, Germany. E-mail: annie.powell@kit.edu

^f Department of Physics, College of Science, Sultan Qaboos University, P.O.Box 50 Al-khod, Oman

^g Department of Physics, University of Kaiserlautern-Landau, Erwin-Schrödinger-Strasse 46, 67663 Kaiserlautern, Germany

bistability. Usually, the coordination environment created by N_4O_2 , $\text{N}_2\text{S}_2\text{O}_2$ and S_6 bring about the SCO nature in Fe(III) complexes, while for Fe(II) , it is N_2O_4 and N_6 .¹² As mentioned above, this kind of a desired coordination environment can bring about by a simple Schiff base condensation *via* an imine linkage from selected primary amines and aldehydes. A search through the recent literature proves that there are some reports on iron(III) complexes with the N_4O_2 coordination environment,^{13–17} where, intramolecular hydrogen or halogen bonding occurs and exhibiting SCO behaviour.

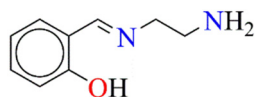
Iron(III) complexes of the Schiff base ligand formed by condensation of ethylenediamine with salicylaldehyde and its substituted derivatives (salen) have been well documented in the literature with some of them showing SCO behaviour.^{18–20} However, comparatively little is known about the asymmetrical Schiff bases of salen origin such as the ligand used in this work (saen) (Scheme 1) and their metal complexes.^{21–24} The structural and magnetic properties of Fe(III) ,^{21,22} Cr(III) ²³ and Co(III) ²⁴ complexes using unsymmetrical salen type ligands have been previously reported. These compounds are closely related to slight variations in terms of counter anion and lattice solvent compared with the present report. One of the Fe(III) complexes reported²² bears a clear structural resemblance to the complex presented here with the exception of the counter anion (chloride in the reported compound and nitrate here) and the lattice solvent (water in the reported compound and MeOH here). The effective magnetic moment at room temperature of the literature known complex²² is in accordance with the LS state in the hydrated form, while HS in the anhydrous species of both chlorido and iodido species, clearly indicating the influence of hydrogen and halogen bonding on the magnetic behaviour of the compound. It is noteworthy that the importance of intermolecular interactions mediated by interactions such as hydrogen and halogen bonding has been shown in a number of SCO systems.^{16,17}

Herein, we report an analogous Fe(III) complex, which is the mixture of both solvated and non-solvated species, *viz.* $[\text{Fe}(\text{saen})_2]\text{NO}_3 \cdot \text{CH}_3\text{OH}$ and $[\text{Fe}(\text{saen})_2]\text{NO}_3$, and has nitrate instead of chloride as counteranion as well as a methanol molecule in the crystal lattice instead of water compared to the previous report²² that was subsequently investigated for its SCO behavior (Scheme 2).

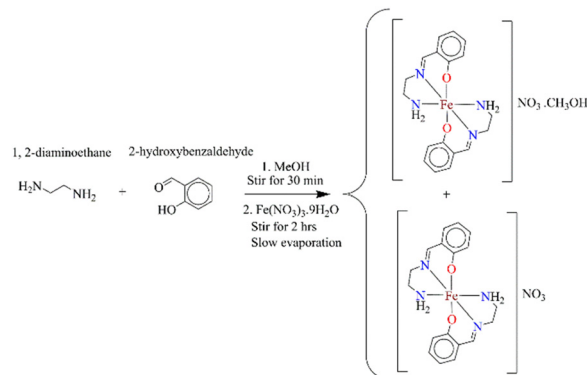
Experimental

Materials

All chemicals and reagents were of analytical grade, purchased from commercial sources and were used without further purification. The FTIR spectrum was measured on a Perkin-Elmer Spectrum 400 in the $4000\text{--}400\text{ cm}^{-1}$ range. Single crystal



Scheme 1 The asymmetric Schiff base ligand saen formed *in situ* through the condensation of salicylaldehyde and ethylenediamine.



Scheme 2 Schematic representation for the formation of complexes **1** and **2**.

XRD measurements were performed on Xcalibur and Gemini diffractometers. Magnetic susceptibility measurements were carried out on an MPMS-3 SQUID magnetometer, operating between 300 and 5 K with an applied magnetic field of 0.1 T. Mössbauer spectroscopy was performed in transmission geometry in the time-scale mode in conjunction with a 512-channel analyzer (WissEl GmbH, Starnberg, Germany). A continuous flow cryostat was used to perform variable temperature measurements (Optistat^{DN}, Oxford Instruments, Abingdon, UK). The radioactive source consisted of ^{57}Co diffused in Rh with an activity of 1.67 GBq and calibration of the spectrometer was conducted against α -iron at room temperature. The spectral data were analyzed using least-squares fits and Lorentzian line shapes employing the public domain program Vinda running on an Excel 2003[®] platform.

Synthesis of the complexes $[\text{Fe}(\text{saen})_2]\text{NO}_3 \cdot \text{CH}_3\text{OH}$ (**1**) and $[\text{Fe}(\text{saen})_2]\text{NO}_3$ (**2**)

A solution of $\text{Fe}(\text{NO}_3)_3 \cdot 9\text{H}_2\text{O}$ (0.404 g, 1 mmol) in 10 ml of methanol was added dropwise into a stirred methanolic solution of salicylaldehyde (0.106 ml, 1 mmol) and ethylenediamine (0.676 ml, 1 mmol) (15 ml). The resultant mixture was stirred for a further 2 h. The brown solution so obtained was filtered and allowed to slowly evaporate at room temperature. Black block-shaped crystals suitable for X-ray diffraction are obtained after two weeks. Yield: 0.36 g, 50%. FTIR (cm^{-1}): 3221 (m), 3141 (m), 1624 (s), 1596 (s), 1541 (m), 1467 (m), 1438 (s), 1365 (m), 1337 (s), 1299 (s), 1196 (m), 1028 (m), 927 (w), 890 (m), 857 (w), 824 (w), 794 (m), 759 (s), 618 (m), 556 (m), 511 (w), 474 (m), 456 (m), 432 (w), 408 (m) (Fig. S1, ESI[†]).

Results and discussion

Synthesis and identification

The mixture of $[\text{Fe}(\text{saen})_2]\text{NO}_3 \cdot \text{CH}_3\text{OH}$ (**1**) and $[\text{Fe}(\text{saen})_2]\text{NO}_3$ (**2**) was prepared by reacting hydrated ferric nitrate with salicylaldehyde and ethylenediamine in methanol and was crystallised *via* slow evaporation of the resultant reaction mixture. The asymmetrical Schiff base formed *in situ* during the reaction coordinates to the Fe(III) centre in a tridentate fashion through the azomethine nitrogen, the primary amine group as well as the

Table 1 Crystal data and structure refinement for complexes **1–173**, and **1–299** and **2**

	1–173	1–299	2
Empirical formula	C ₁₉ H ₂₆ FeN ₅ O ₆	C ₁₉ H ₂₆ FeN ₅ O ₆	C ₁₈ H ₂₂ FeN ₅ O ₅
Formula weight	476.30	476.30	444.25
Temperature/K	173(2)	299(2)	173(2)
Crystal system	Monoclinic	Monoclinic	Triclinic
Space group	<i>Cc</i>	<i>Cc</i>	<i>P</i> $\bar{1}$
<i>a</i> /Å	7.59350(10)	7.5856(5)	9.5094(4)
<i>b</i> /Å	25.7764(7)	25.835(2)	9.7005(4)
<i>c</i> /Å	10.7145(3)	10.6741(7)	10.5055(5)
α /°	90	90	90.837(3)
β /°	95.798(2)	95.694(7)	92.565(3)
γ /°	90	90	97.079(3)
Volume/Å ³	2086.45(9)	2081.5(3)	960.54(7)
<i>Z</i>	4	4	2
ρ_{calc} g cm ^{−3}	1.516	1.52	1.536
μ mm ^{−1}	0.770	0.772	0.827
<i>F</i> (000)	996	996	462
Crystal size/mm ³	0.51 × 0.37 × 0.28	0.46 × 0.32 × 0.12	0.59 × 0.34 × 0.20
Wavelength/Å	0.71073	0.71073	0.71073
θ range for data collection/°	3.161 to 29.689	2.811 to 29.307	2.901 to 28.986
Index ranges	10 ≤ <i>h</i> ≤ 10 35 ≤ <i>k</i> ≤ 35 14 ≤ <i>l</i> ≤ 14	10 ≤ <i>h</i> ≤ 9 30 ≤ <i>k</i> ≤ 33 10 ≤ <i>l</i> ≤ 14	12 ≤ <i>h</i> ≤ 12 13 ≤ <i>k</i> ≤ 12 13 ≤ <i>l</i> ≤ 13
Reflections collected	24 876	5113	12 484
Independent reflections	5390 [<i>R</i> (int) = 0.0415]	3253 [<i>R</i> (int) = 0.0230]	4498 [<i>R</i> (int) = 0.0316]
Data/restraints/parameters	5390/2/282	3253/2/282	4498/0/268
Goodness-of-fit on <i>F</i> ²	1.068	1.079	1.061
Final <i>R</i> indexes [<i>I</i> > = 2σ(<i>I</i>)]	<i>R</i> ₁ = 0.0387 <i>wR</i> ₂ = 0.0769	<i>R</i> ₁ = 0.0422 <i>wR</i> ₂ = 0.1206	<i>R</i> ₁ = 0.0448 <i>wR</i> ₂ = 0.0983
Final <i>R</i> indexes [all data]	<i>R</i> ₁ = 0.0549 <i>wR</i> ₂ = 0.0840	<i>R</i> ₁ = 0.0441 <i>wR</i> ₂ = 0.1231	<i>R</i> ₁ = 0.0694 <i>wR</i> ₂ = 0.1088
Largest diff. peak/hole/e Å ^{−3}	0.365 and 0.263	0.296 and 0.312	0.464 and 0.302

deprotonated phenolate oxygen. Similar structural motifs were reported by Feng *et al.*²¹ and Summerton *et al.*,²² and these compounds only differ from the present complexes regarding the counter anion and solvate molecules. However, in contrast to the previous reports, the present complex was prepared by generating the Schiff base ligand under *in situ* conditions.

Crystal structures of **1** and **2**

As mentioned above the crystal structure of **1** was determined at two temperatures, at 173 K (**1–173**) and at 299 K (**1–299**) with the aim to check for possibility of phase transition. The results have shown that the structure at both temperatures is essentially the same with minor changes in geometric parameters which can be attributed to the difference in temperatures (Fig. 1 and Table 1). As can be seen from this Fig. 1, the thermal ellipsoids at 299 K are large as the corresponding ones measured at 173 K as expected.

The molecular structure of the title complex consists of the cationic [Fe(saen)₂]⁺ moiety, a nitrate anion and one methanol molecule in the lattice. The central Fe(III) ion is coordinated by two tridentate ligands formed by the deprotonation of the Schiff base ligand saen. A search in the crystallographic database CSD reveals that analogous Fe(III) complexes with a thiocyanate [Fe(L)₂](SCN)²¹ and chloride counteranion [Fe(L)₂](Cl)·H₂O²² were previously reported. Here, in both studied temperatures, the Fe(III) exhibits a slightly distorted octahedral N₄O₂ coordination geometry with the two phenolate oxygens from the saen ligand *cis* to each other (Fig. S2, ESI†)

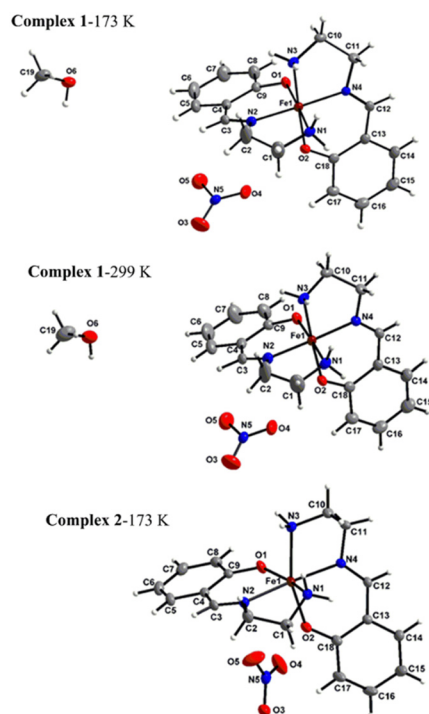


Fig. 1 Thermal ellipsoid plots of the complex **1–173** (upper), **1–299** (middle) and **2** (bottom). The hydrogen atoms are not labelled for clarity. The thermal ellipsoids are drawn at the 30% probability level.

Table 2 Selected bond distances and bond angles [\AA , $^\circ$] for complexes **1–173**, **1–299** and **2**

	1–173	1–299	2
Fe1–O1	1.877(3)	1.886(4)	1.9151(17)
Fe1–O2	1.894(2)	1.878(4)	1.9204(17)
Fe1–N1	2.002(4)	1.998(4)	2.184(2)
Fe1–N2	1.926(3)	1.927(5)	2.1277(18)
Fe1–N3	2.004(3)	2.011(5)	2.198(2)
Fe1–N4	1.922(3)	1.937(4)	2.1107(18)
O1–Fe1–O2	93.27(11)	93.39(18)	101.31(8)
O1–Fe1–N2	93.34(12)	93.14(19)	86.68(7)
N1–Fe1–N2	84.42(13)	84.5(2)	76.59(7)
O2–Fe1–N4	94.59(12)	94.26(16)	86.16(7)
N3–Fe1–N4	83.84(14)	83.6(2)	77.18(7)

as corroborated by the calculations using the SHAPE program²⁵ (Table S1, ESI†).

The two tridentate Schiff-base ligands **L** are coordinated in *mer*-fashion. The Fe–O and Fe–N bond distances in **1** (Table 2) are in rather narrow ranges 1.877(3)–1.894(2) \AA and 1.922(3)–2.004(3) \AA , respectively, at 173 K and 1.886(4) \AA –1.878(4) and (1.937(4)–2.011(5) \AA), respectively, at 299 K. These distances are similar to those found in the analogous thiocyanate and chloride complexes.^{21,22} The obtained angles in **1** are close to 90 degrees, which confirm the quite regular octahedral coordination of the Fe(III) central atom in **1** at both temperatures.

The nitrate anion, besides balancing the positive charge of the complex cation, plays an important role in the construction of the supramolecular structure in **1**. The nitrate anion is involved in hydrogen bonds of the N–H \cdots O type (Table 3 and Table S2, ESI†) linking neighbouring complex cations in a supramolecular chain. These chains are interconnected by methanol solvate molecules *via* hydrogen bonds of the N–H \cdots O and O–H \cdots O types yielding supramolecular sheets in the *ac* plane (Fig. 2). No interlayer interactions were found between these supramolecular sheets. The shortest distance between the neighboring Fe1 and Fe1ⁱⁱⁱ (iii: 1 + *x*, *y*, *z*) atoms is 7.594 \AA at

173 K and 7.586(1) \AA at 299 K, which is too far for any considerable magnetic exchange interaction.

The crystal structure of **2** is the same as the crystal structure of **1** but without the methanol solvate molecule: it is composed of [Fe(saen)₂]⁺ complex cations and nitrate anions (Fig. 1 bottom). Within the complex cation the Fe(III) central atom exhibits the same type of coordination as in **1**. On the other hand, the obtained geometric parameters significantly differ from the corresponding **1** at 173 K (Table 2). The Fe–O bonds in **2** are slightly longer with a mean value of 1.918 \AA , compared to 1.886 \AA in **1** at 173 K. The Fe–N bond distances are longer in **2** compared with that in **1** at 173 K, with a mean value of 2.155 \AA in **2** while 1.964 \AA in **1**. Such longer Fe(III)–O and Fe(III)–N bonds have already been reported, in [Fe(sal-tet)]ClO₄; sal-tet = *N,N'*-bis(2-(salicylideneamino)ethyl)-1,3-diaminopropane), with mean values of Fe–O and Fe–N bonds being 1.925 \AA and 2.171 \AA , respectively²⁶ and in the [Fe^{III}(L2)]ClO₄ complex (L2 = 2,2'-(2,5,9,12-tetraazatrideca-1,12-diene-1,13-diyl)bis(3,5-dimethoxyphenolato), which is in the HS state, the mean values are 1.906 and 2.095 \AA .²⁷ Furthermore, the bond lengths for forms **1** and **2** fall within the ranges observed for LS and HS Fe(III) complexes, respectively.²⁸

The coordination polyhedron in **2** is somewhat more deformed as in **1–173** as seen in Fig. S2, ESI† and on the overlay of the two complex cations in Fig. S3, ESI†. The deformation of the coordination polyhedron manifests itself *via* X–Fe–X (X is the donor atom) angles, which deviate more from the right-angle value as in **1–173**. Results of the SHAPE program²⁵ calculations corroborate a slightly higher deformation of the Fe(III) central atom polyhedron (Table S1, ESI†).

In the crystal structure of **2** and likewise that of **1**, the supramolecular structure is governed by hydrogen bonds of the NH \cdots O types linking the complex cations and nitrate anions in a zig-zag 1D arrangement running along the *a* axis (Fig. 3 and Table 4). The supramolecular ladders formed are additionally linked by much weaker hydrogen bonding interactions of the C–H \cdots O type. The shortest distance between the Fe1 atom and

Table 3 Possible hydrogen bonds for **1–173** (upper) and **1–299** (bottom)

D–H \cdots A	<i>d</i> (D \cdots H)	<i>d</i> (H \cdots A)	<i>d</i> (D \cdots A)	<(DHA)
N1–H1C \cdots O6 ⁱ	0.91	2.17	3.036(4)	158
N1–H1D \cdots O3 ⁱⁱ	0.91	2.45	3.195(5)	140
N1–H1D \cdots O5 ⁱⁱ	0.91	2.33	3.223(5)	166
N3–H3C \cdots O4 ⁱⁱⁱ	0.91	2.01	2.912(5)	173
N3–H3D \cdots O5 ⁱⁱ	0.91	2.10	2.925(5)	150
O6–H6O \cdots O1 ^{iv}	0.84(4)	1.93(4)	2.752(4)	167(5)
Symmetry transformations used to generate equivalent atoms: (i) <i>x</i> – 1/2, <i>y</i> + 1/2, <i>z</i> + 1/2; (ii) <i>x</i> + 1/2, <i>y</i> + 1/2, <i>z</i> + 1/2; (iii) <i>x</i> + 1, <i>y</i> , <i>z</i> ; (iv) <i>x</i> – 1/2, <i>y</i> + 1/2, <i>z</i> – 1/2.				
D–H \cdots A	<i>d</i> (D \cdots H)	<i>d</i> (H \cdots A)	<i>d</i> (D \cdots A)	<(DHA)
T = 299 K				
N1–H1C \cdots O6 ⁱⁱ	0.89	2.24	3.084(7)	159
N1–H1D \cdots O3 ⁱⁱⁱ	0.89	2.44	3.174(8)	140
N1–H1D \cdots O5 ⁱⁱⁱ	0.89	2.36	3.231(7)	167
N3–H3D \cdots O4 ^{iv}	0.89	2.04	2.927(7)	173
N3–H3C \cdots O5 ⁱⁱⁱ	0.89	2.12	2.929(7)	151
O6–H6O \cdots O1 ⁱ	0.82(4)	1.96(4)	2.775(6)	176(5)
Symmetry transformations used to generate equivalent atoms: (i) <i>x</i> – 1/2, <i>y</i> + 1/2, <i>z</i> – 1/2; (ii) <i>x</i> – 1/2, <i>y</i> + 1/2, <i>z</i> + 1/2; (iii) <i>x</i> + 1/2, <i>y</i> + 1/2, <i>z</i> + 1/2; (iv) <i>x</i> + 1, <i>y</i> , <i>z</i> .				

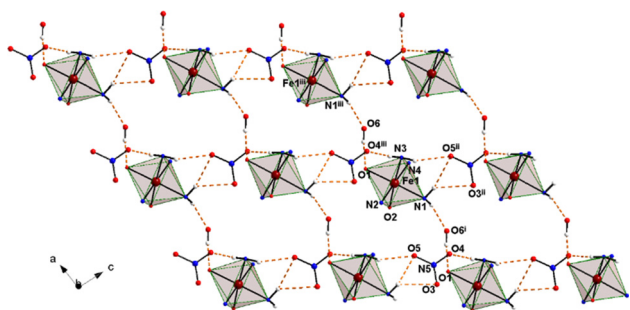


Fig. 2 View on the hydrogen bonding system in **1**–**173**. For the sake of clarity, carbon atoms and hydrogen atoms not involved in hydrogen bond formation are omitted. Symmetry codes: (i) $x - 1/2, -y + 1/2, z + 1/2$; (ii) $x + 1/2, -y + 1/2, z + 1/2$; (iii) $x + 1, y, z$.

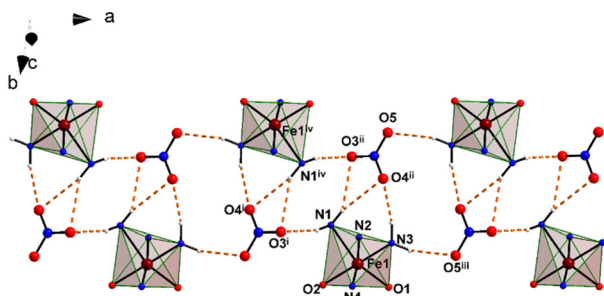


Fig. 3 View of the hydrogen bonding system in **2**. For the sake of clarity, carbon atoms and hydrogen atoms not involved in hydrogen bond formation are omitted. Symmetry codes: (i) $1 - x, 1 - y, 1 - z$; (ii) $x, y - 1, z - 1$; (iii) $2 - x, 1 - y, 1 - z$; (iv) $1 - x, -y, -z$.

Table 4 Possible hydrogen bonds for **2**

D–H···A	$d(\text{D} \cdots \text{H})$	$d(\text{H} \cdots \text{A})$	$d(\text{D} \cdots \text{A})$	$\angle(\text{DHA})$
N1–H1C···N5 ⁱⁱⁱ	0.91	2.70	3.487(3)	146
N1–H1C···O3 ⁱⁱⁱ	0.91	2.08	2.973(3)	166
N1–H1D···O3 ^{iv}	0.91	2.47	3.224(3)	140
N1–H1D···O4 ^{iv}	0.91	2.55	3.443(3)	168
N3–H3C···O5 ⁱ	0.91	2.46	3.135(3)	132
N3–H3D···O4 ^{iv}	0.91	2.18	2.985(3)	147

Symmetry transformations used to generate equivalent atoms: (i) $x + 2, y + 1, z + 1$; (ii) $x, y, z - 1$; (iii) $x + 1, y + 1, z + 1$; (iv) $x, y - 1, z - 1$.

its symmetry related congener Fe1^{iv} (iv: $1 - x, -y, -z$) is 7.911 Å; these iron atoms are linked by a centrosymmetric system of hydrogen bonds along the path Fe–N–H···O···H–N–Fe.

PXRD analysis

Powder X-ray diffraction pattern (PXRD) of a fresh sample of the compound at room temperature shows the presence of both the [Fe(saen)₂]₂NO₃·CH₃OH (**1**) monoclinic and the [Fe(saen)₂]₂NO₃ (**2**) triclinic form (Fig. S3, ESI[†]).

Sample preparation for both the SQUID and Mössbauer experiments which are discussed in the following involved vigorous grinding (trituration) which resulted in complete desolvation of the compound leading to a pure batch of form (**2**).

Table 5 Mössbauer parameters of compound **1** as obtained from the analysis displayed in Fig. 5

Temperature Component	77 K	175 K		300 K	
		1	2	1	2
δ (mm s ^{−1})	0.20(5)	0.16(5)	0.89(5)	0.12(5)	0.86(4)
ΔE_Q (mm s ^{−1})	2.90(4)	0.00(4)	0.00(5)	0.00(4)	0.00(5)
Γ (mm s ^{−1})	0.40(4)	0.70(5)	2.10(5)	0.60(5)	1.42(4)
Rel. area (%)	100	50	50	50	50

Temperature dependent magnetic properties

The investigation of the temperature dependence of the magnetic susceptibility under an applied dc field of 0.1 T was performed for both warming (↑) and cooling cycles (↓) in the temperature range 5 to 300 K using two different temperature scan rates (3 K min^{−1} and 5 K min^{−1}, as indicated in Fig. 4. The $\chi_M T$ versus T plot of a polycrystalline sample of **1** is shown in Fig. 4.

The room-temperature $\chi_M T$ value of **1** of 4.62 cm³ mol^{−1} K is characteristic of a ⁶A₁ ($S = 5/2$) ground-state for an iron(III) species in an octahedral coordination environment.^{29,30} Upon cooling, the value of $\chi_M T$ abruptly decreases to 0.68 cm³ mol^{−1} K at 80 K and reaches a minimum value of 0.54 cm³ mol^{−1} K at 5 K, proving complete transition to low spin conditions (²T₂, $S = 1/2$) of Fe(III) species with $\chi_M T$ of 0.375 cm³ mol^{−1} K.³⁰ Because of the significant orbital contribution, the $\chi_M T$ value increases up to the value of 4.62 cm³ mol^{−1} K and 0.54 cm³ mol^{−1} K for HS and LS respectively, in compared to the expected values.³⁰ Measurements performed in both heating (↑) and cooling (↓) cycles have revealed the occurrence of a *ca.* 27 K wide steep thermal hysteresis loop ($T_{1/2}$ (↑) = 152 K and $T_{1/2}$ (↓) = 125 K).

The presence of SCO with a wide and steep thermal hysteresis loop clearly proves the influence of the extended hydrogen bond network between amino hydrogens: the nitrate counter anion and methanol molecule in **1** and with nitrate counter anion and amino hydrogens in **2** in the crystal lattice (Fig. 2 and 3). The hydrated chlorido analogue of the complex,²² is in the LS state

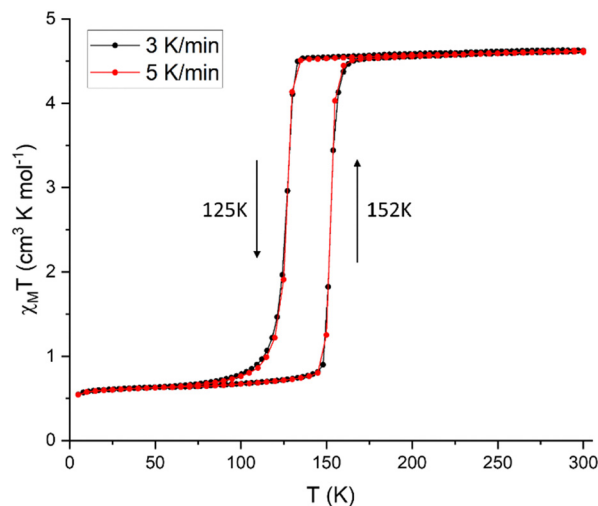


Fig. 4 $\chi_M T$ vs. T plot for a polycrystalline sample of the complex in warming (↑) and cooling (↓) cycles.

at room temperature, where, intramolecular hydrogen and halogen bond connect two complex units. On the other hand, it is in the HS state in the non-hydrated form, where there is no hydrogen and halogen bond occurring in accordance with effective magnetic moment measurements. It is also interesting to note that the non-hydrated iodido derivative is, in HS at room temperature.

Variable temperature Mössbauer spectroscopy

The Mössbauer spectrum of compound **1** taken at 77 K displays a doublet with an isomer shift $\delta = 0.20 \text{ mm s}^{-1}$ and a quadrupole splitting of $\Delta E_Q = 2.90 \text{ mm s}^{-1}$. The relative low value of the isomer shift is characteristic for a ferric low spin system.³¹ The high value of the quadrupole splitting is consistent with an asymmetric charge distribution caused by a $3d^5$ system in an octahedral ligand field with a hole in the almost filled t_{2g} orbitals with a $S = 1/2$ ground state. As no magnetic splitting is observed it can be concluded that the electronic relaxation time is faster than the Larmor precession time of the ^{57}Fe nucleus in the magnetic hyperfine field of the ferric low spin system. When the temperature is raised to 175 K the Mössbauer spectrum changes completely and turns into a relatively broad asymmetric doublet with $\delta = 0.52 \text{ mm s}^{-1}$ and $\Delta E_Q = 0.73 \text{ mm s}^{-1}$. These parameters are characteristic for a ferric high spin state.³² The spectrum is broadened because of the magnetic relaxation effects of the $S = 5/2$ system. In contrast to the $S = 1/2$

state the electronic spin relaxation time of the $S = 5/2$ state is still within the range of the Larmor precession time of the ^{57}Fe nucleus. Such a situation is called the case of intermediate relaxation³³ and has been modelled here by simulation of the spectral data with an asymmetric doublet having different line widths. The overall pattern of the Mössbauer spectrum does not change much when measured at 300 K. The slight decrease of the isomer shift to $\delta = 0.43 \text{ mm s}^{-1}$ is due to the second order Doppler shift and the line widths of the asymmetric spectrum are decreased pointing to an accelerated spin relaxation rate due to spin lattice relaxation. In conclusion the Mössbauer spectroscopic data are fully consistent with the susceptibility data (Fig. 4) and unambiguously show that compound **1** undergoes temperature induced SCO from $S = 1/2$ to $S = 5/2$ (Fig. 5).

Conclusions

In summary, we have synthesised and characterised asymmetrical iron(III) Schiff base complexes from ethylenediamine and salicylaldehyde under *in situ* conditions and subsequently characterised by FT-IR and single crystal XRD studies. The asymmetrical ligand generated during the *in situ* synthesis, coordinated to the central metal ion through the deprotonated phenolate oxygen, azomethine as well as amino nitrogens. The two molecules of the ligand wrap around the central Fe(III) atom generating an octahedral geometry with the nitrate counter anion. The complexes crystallised as a mixture of two fractions, one with solvated methanol and the other without, having intramolecular hydrogen bonding between the complex molecules either through methanol and nitrate anion in the solvated variety or nitrate anion alone in the non-solvated form through amino hydrogens.

The magnetic properties of the present complex in its solvated and desolvated forms are consistent with those of a previously reported halide salt of the analogous Fe(III) complex, for which it was also observed that the hydrated form was LS whereas the non-hydrated form was HS at room temperature.²² The temperature-dependent magnetic and Mössbauer measurements were both carried out on thoroughly ground samples which led to pure batches of form (2). These magnetic measurements show that the compound exhibits abrupt SCO behaviour with a hysteresis width of 27 K, which is supported by variable temperature Mössbauer spectral studies at 77, 175 and 300 K.

Author contributions

Dawit Tesfaye: design, synthesis, conceptualisation, methodology, formal analysis, investigation, and writing the original draft which is part of his PhD program; Mamo Gebrezgiabher: formal analysis, co-investigation, writing and editing; Jonas Braun: characterisation (SQUID measurement and analysis), review and editing; Tajū Sani: data curation; Abbasher Gismelseed, Tim Hochdörffer and Volker Schünemann: Mössbauer measurements; Juraj Kuchár: crystallography; Juraj Černák: crystallography; Christopher E. Anson: editing and reviewing; Madhu Thomas: supervision, editing and reviewing and funding acquisition;

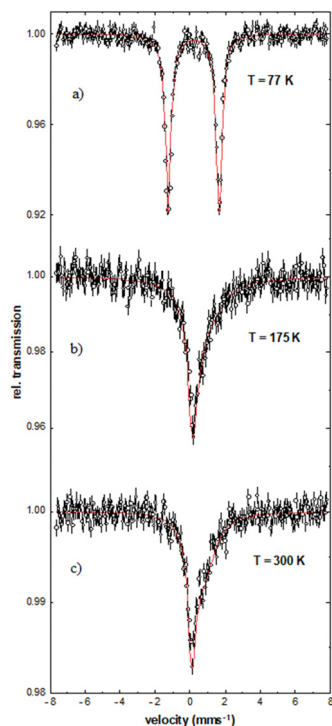


Fig. 5 Mössbauer spectra of compound **1** at (a) 77 K, (b) 175 K and (c) 300 K. The open circles display the experimental data obtained at the denoted temperature and the red solid lines represent simulations using Lorentzian line shape. The spectra obtained at 175 and 300 K are broadened by relaxation effects. They have been analyzed with an asymmetric doublet and different line width at half maximum Γ . The parameters of the simulations are listed in Table 5.

Annie K. Powell: supervision, editing and reviewing the article as well as funding acquisition.

Data availability

Crystallographic data for compounds are deposited in the Cambridge Crystallographic Data Centre, CCDC no. 2343431 (1–173), 2343432 (1–299) and 2343433 (2).[†]

Conflicts of interest

There are no conflicts to declare.

Acknowledgements

This work was supported by the Scientific Grant Agency of Ministry of Education, Science, Research and Sport of the Slovak Republic (contract no. VEGA 1/0189/22). V. S. acknowledges support from the German Ministry of Research (BMBF) under 05K22UK1. J. B., C. E. A. and A. K. P. acknowledge funding from the Helmholtz Foundation POF MSE. D. T. is thankful to the Slovakian National Scholarship Programme (2023) for a short research stay and the Salale University, Addis Ababa Science and Technology University, Ethiopia for PhD studentship. The financial support from the internal research grants (IG 07/2021 and IRG 08/2024) of the Addis Ababa Science and Technology University is also thankfully acknowledged.

Notes and references

- 1 L. Cambi and L. Szegö, *Ber. Dtsch. Chem. Ges.*, 1931, **64**, 2591–2598.
- 2 A. Bousseksou, K. Boukheddaden, M. Goiran, C. Consejo, M. L. Boillot and J. P. Tuchagues, *Phys. Rev. B: Condens. Matter Mater. Phys.*, 2002, **65**, 172412.
- 3 Y. Garcia, V. Ksenofontov, G. Levchenko, G. Schmitt and P. Gutlich, *J. Phys. Chem. B*, 2000, **104**, 5045–5048.
- 4 G. Matouzenko and A. Bousseksou, *Eur. J. Inorg. Chem.*, 2004, 4353–4369.
- 5 P. Gütlich, C. P. Köhler, H. Spiering and A. Hauser, *Chem. Phys. Lett.*, 1984, **105**, 3–6.
- 6 D. Tesfaye, W. Linert, M. Gebrezgiabher, Y. Bayeh, F. Elemo, T. Sani, N. Kalarikkal and M. Thomas, *Molecules*, 2023, **28**, 1012.
- 7 K. Senthil Kumar, Y. Bayeh, T. Gebretsadik, F. Elemo, M. Gebrezgiabher, M. Thomas and M. Ruben, *Dalton Trans.*, 2019, **48**, 15321–15337.
- 8 H. Schiff, *Justus Liebig's Ann. Chem.*, 1864, **131**, 118–119.
- 9 N. T. Madhu, J. K. Tang, I. J. Hewitt, R. Clérac, W. Wernsdorfer, J. Van Slageren, C. E. Anson and A. K. Powell, *Polyhedron*, 2005, **24**, 2864–2869.
- 10 J. Braun, D. Seufert, C. E. Anson, J. Tang and A. K. Powell, *Int. J. Mol. Sci.*, 2024, **25**, 4–11.
- 11 M. Gebrezgiabher, Y. Bayeh, T. Gebretsadik, G. Gebreslassie, F. Elemo, M. Thomas and W. Linert, *Inorganics*, 2020, **8**, 66.
- 12 P. Gütlich and H. A. Goodwin, *Top. Curr. Chem.*, 2012, **1**, 1–47.
- 13 R. T. Marques, L. P. Ferreira, C. S. B. Gomes, C. S. D. Lopes, C. E. S. Bernardes, N. K. Sarangi, T. E. Keyes and P. N. Martinho, *Cryst. Growth Res.*, 2023, **23**, 3222–3229.
- 14 P. N. Martinho, I. A. Kühne, B. Gildea, G. McKerr, B. O'Hagan, T. E. Keyes, T. Lemma, C. Gandolfi, M. Albrecht and G. G. Morgan, *Magnetochemistry*, 2018, **4**, 49.
- 15 B. Dey, A. Mondal and S. Konar, *Chem. – Asian J.*, 2020, **15**, 1709–1721.
- 16 R. Busch, A. B. Carter, K. F. Konidaris, I. A. Kühne, R. González, C. E. Anson and A. K. Powell, *Chem. – Eur. J.*, 2020, **26**, 11835–11840.
- 17 S. Sundaresan, I. A. Kühne, C. T. Kelly, A. Barker, D. Salley, H. Müller-Bunz, A. K. Powell and G. G. Morgan, *Crystals*, 2018, **9**, 19.
- 18 A. Earnshaw, E. A. King and L. F. Larkworthy, *J. Chem. Soc. A*, 1969, 2459–2463.
- 19 A. Earnshaw, E. A. King and L. F. Larkworthy, *Chem. Commun.*, 1965, 180.
- 20 F. V. Wells, S. W. McCann, H. H. Wickman, S. L. Kessel, D. N. Hendrickson and R. D. Feltham, *Inorg. Chem.*, 1982, **21**, 2306–2311.
- 21 X. Feng, X. Han and L. Wang, *Z. Kristallogr. – New Cryst. Struct.*, 2006, **221**, 296–298.
- 22 A. P. Summerton, A. A. Diamantis and M. R. Snow, *Inorg. Chim. Acta*, 1978, **27**, 123–128.
- 23 A. P. Gardner, B. M. Gatehouse and J. C. B. White, *Acta Crystallogr., Sect. B: Struct. Crystallogr. Cryst. Chem.*, 1971, **27**, 1505–1509.
- 24 T. H. Benson, M. S. Bilton and N. S. Gill, *Aust. J. Chem.*, 1977, **30**, 261–270.
- 25 M. Llunell, D. Casanova, J. Cirera, P. Alemany and S. Alvarez, *SHAPE. Program for the Stereochemical Analysis of Molecular Fragments by Means of Continuous Shape Measures and Associated Tools*, University of Barcelona, Barcelona, 2013.
- 26 S. Hayami, T. Matoba, S. Nomiyama, T. Kojima, S. Osaki and Y. Maeda, *Bull. Chem. Soc. Jpn.*, 1997, **70**, 3001–3009.
- 27 M. Griffin, S. Shakespeare, H. J. Shepherd, C. J. Harding, J. F. Létard, C. Desplanches, A. E. Goeta, J. A. K. Howard, A. K. Powell, V. Mereacre, Y. Garcia, A. D. Naik, H. Müller-Bunz and G. G. Morgan, *Angew. Chem., Int. Ed.*, 2011, **50**, 896–900.
- 28 M. S. Shongwe, B. A. Al-Rashdi, H. Adams, M. J. Morris, M. Mikuriya and G. R. Hearne, *Inorg. Chem.*, 2007, **46**, 9558–9568.
- 29 Y. Ikuta, M. Ooidemizu, Y. Yamahata, M. Yamada, S. Osa, N. Matsumoto, S. Iijima, Y. Sunatsuki, M. Kojima, F. Dahan and J. P. Tuchagues, *Inorg. Chem.*, 2003, **42**, 7001–7017.
- 30 J. Tang, J. S. Costa, S. Smulders, G. Molnár, A. Bousseksou, S. J. Teat, Y. Li, G. A. Van Albada, P. Gamez and J. Reedijk, *Inorg. Chem.*, 2009, **48**, 2128–2135.
- 31 T. Teschner, L. Yatsunyk, V. Schünemann, H. Paulsen, H. Winkler, C. Hu, W. R. Scheidt, F. A. Walker and A. X. Trautwein, *J. Am. Chem. Soc.*, 2006, **128**, 1379–1389.
- 32 V. Schünemann and H. Winkler, *Rep. Prog. Phys.*, 2000, **63**, 263–353.
- 33 S. Mørup, *Magnetic Relaxation Phenomena*, in *Mössbauer Spectroscopy and Transition Metal Chemistry*, Springer, Berlin, Heidelberg, 2011, pp. 209–234.